



ASHESI UNIVERSITY

PIEZOELECTRIC GLOVE SENSOR FOR EARLY DETECTION

CAPSTONE PROJECT

B.Sc. Electrical & Electronics Engineering

Kristen Frimponmah Agyeman-Prempeh

2021

ASHESI UNIVERSITY

PIEZOELECTRIC GLOVE SENSOR FOR EARLY DETECTION

CAPSTONE PROJECT

Capstone Project submitted to the Department of Engineering, Ashesi University
in partial fulfilment of the requirements for the award of Bachelor of Science
degree in Electrical & Electronics Engineering.

Kristen Frimponmah Agyeman-Prempeh

2021

DECLARATION

I hereby declare that this capstone is the result of my own original work and that no part of it has been presented for another degree in this university or elsewhere.

Candidate's Signature:

.....K.A.P.....

Candidate's Name:Kristen Frimponmah Agyeman-Prempeh.....

Date: Tuesday, April 27, 2021.....

I hereby declare that preparation and presentation of this capstone were supervised in accordance with the guidelines on supervision of capstone laid down by Ashesi University College.

Supervisor's Signature:

.....

Supervisor's Name:

.....

Date:

.....

Acknowledgements

Being confident of this very thing, that he which hath begun a good work in you will perform it until the day of Jesus Christ.

~Philippians 1:6

I would first love to thank God for His faithfulness and unending love towards me. He granted me guidance in this four-year journey and the grace to will and to do this project. He who started this good work in me has seen it come to a glorious end.

To my supervisor, Dr. Elena Rosca, I have been truly overwhelmed by your support and selfless guidance, which directed me on the path to excellence. Thank you for giving me the opportunity to work with and under you on this project. I could not have completed this project without your sincerity and the wealth of knowledge you shared.

My utmost gratitude and love go to my parents - Rev. and Mrs. Agyeman-Prempeh, my siblings and their families: Akwasi, Rev Denzel, Rev. Nana Opoku, Daisy, Prophet'16, Samuel'19, and Michael'21, for their endless support in finances, motivation, correction, and love to persevere and be exceptional in all things. Special thanks to Mr. Alexander Owusu-Ansah & family, Apostle Kingsley Ajei-Godson & family, Mr. Patrick Dwomfuor, Dr. Joseph Clottey, Kwasi Osei-Kusi, and Mrs. Elormrita Bansah, for being a great source of motivation and strong pillars in my Ashesi journey and beyond.

Finally, to the Kingdom Christian Fellowship family and the Ashesi family, my association and relationship with you have been the best gift ever received in Ashesi. Your constant prayers, laughs, and stories shared have shaped me into the person I am today, and I will always cherish these memories. Thank you, Ashesi University, for training and raising me as an ethical citizen and leader in Africa.

Abstract

Breast cancer is the top cancer in women in the developed and the developing world. Globally, about 25% and 15% of all new cancer cases and cancer deaths, respectively, among females were due to breast cancer[2]. According to the American Cancer Society, when breast cancer is detected early and is in the localized stage, the 5-year relative survival rate is 99% [3]. Early detection is enhanced by conducting monthly breast self-exams. However, these existing screening methods, such as MRI, Mammography, and Ultrasound, are expensive, making it difficult for the masses to conduct self-examination regularly. As a result, women in low and middle-income countries suffer the most due to breast cancer.

This project seeks to develop a cost-effective system for detecting breast cancer cells in stages 0 and 1(*early-stage detection*) through tissue stiffness, which contrasts with the traditional mechanical or optical means of detection. It has been identified that the stiffness of a normal breast tissue is less than that of a malignant tissue. Therefore, by determining the elasticity of the breast tissue, it can be deduced if a tumor has been detected in the breast.

The piezoelectric glove sensor combines the traditional method of self-examination: clinical breast examination (CBE) to conduct examinations. Three tests were conducted on three breast phantoms containing four tumors of different sizes using the glove sensor. The system was able to detect some of these tumors placed in the breast phantom. The sensitivity and specificity of the system were 84.6% and 83.3% respectively, concluding that the piezoelectric glove has a sensitivity and specificity more significant than a Mammogram and CT scan, and therefore is a suitable pre-screening device for early detection.

Table of Contents

DECLARATION	i
Acknowledgements	ii
Abstract	iii
List of Tables.....	vii
List of Figures	vii
Equations.....	viii
Code Listings	ix
Chapter 1: Introduction	1
1.1 Background: Breast Cancer in Africa	1
1.2 Problem Definition.....	2
1.3 Project Aims & Objectives.....	3
Chapter 2: Literature Review	4
2.1 Breast Cancer Overview	4
2.1.1 Breast Cancer Stages.....	5
2.2 Breast Cancer Imaging Procedures	6
Chapter 3: System Requirements & Innovative Design	10
3.1 Hardware and Software Requirements.....	10
3.1.1 Hardware Requirements:.....	10
3.1.2 Software Requirements:	11

3.2	System Design and Device Selection.....	11
3.2.1	System Design:	11
3.2.2	Device Selection.....	13
Chapter 4: Implementation, Testing & Results.....		18
4.1	Modeling of the Breast and Tumor Phantoms	18
4.1.1	Methodology and Measurements	18
4.2	Implementation	19
4.2.1	Schematic Diagram and Breadboard Representation of the Circuit.	20
4.3	Testing & Recording:.....	24
4.3.1	Amplification and Filtering test:	24
4.3.2	Piezo sensor test without tissue phantoms:	25
Chapter 5: Results & Discussions		27
Chapter 6: Conclusion.....		29
6.1	Conclusion	29
6.2	Challenges & Limitations.	30
6.3	Future Work & Recommendations	31
APPENDIX A: ADC Code in Keil Uvision		37
APPENDIX B: Serial UART Code for Bluetooth Connection.....		38
APPENDIX C: Code to Execute ADC, Bluetooth data transfer & Light LEDs		40
APPENDIX D:Bill of Materials		45
APPENDIX E:3D modeling of system using Blender.....		46

APPENDIX F: $V_{in,o}$, V_{in} and Elastic mod vals	47
APPENDIX G: Readings from Breast phantom only	48

List of Tables

Table 2.1.1.1 Comparison of the existing breast cancer imaging procedures. [10,19,21]	9
Table 3.2.2.1 Pugh chart analysing the major biosensors which can be used in detecting breast cancer cells.	14
Table 4.1.1.1 Measurement of breast phantoms. The masses approximated based on the weight of the gelatin product used.	19
Table 4.3.2.1 Case Definition [34].....	29

List of Figures

Figure 2.1.1.1 A labelled anatomy of the breast(left). Symptoms of breast cancer (right)	5
--	---

Figure 2.1.1.1 shows the imaging techniques used in detecting cancer cells in the breast.	7
Figure 3.2.1.1 Method of examination (A) and how the system will be operated (B)	12
Figure 3.2.1.2 Block diagram of proposed system.....	13
Figure 3.2.2.1 Analog Ceramic Piezo Vibration Sensor.....	14
Figure 3.2.2.2 is the active low-pass filter with a gain arrangement for amplification	15
Figure 3.2.2.3 The UA741-N operational amplifier	16
Figure 3.2.2.4 NXP FRDM KL25Z Board	17
Figure 3.2.2.5 Bluetooth module (HC-05).....	17
Figure 4.1.1.1 3D modelled system using Blender app (left) and real-life system(right).	20
Figure 4.2.1.1 Bluetooth terminal displaying voltage readings (left) and the schematic diagram & breadboard representation of the system.....	21

Equations

$E = 12\pi A121 - v2[Vin, 0 - VinVin]$ (Equation 3.2.1.1) [19]	13
$fc = 12\pi RC$ (Equation 3.2.2.1)	15
$Concentration = MassVolume$ (Equation 4.1.1.1).....	19
$Volume\ of\ hemisphere = 23\pi r^3$ (Equation 4.1.1.2).....	19

Sensitivity = $AA + C$, Equation 4.3.2.2 [34]	28
<i>Specificity = $DD + B$, Equation 4.3.2.3 [34]</i>	29

Code Listings

Code 4.2.1.1 Code snippet performing ADC	21
Code 4.2.1.2 Code snippet setting up serial Bluetooth connection.....	22
Code 4.2.1.3 On-board LED setup and Control.....	23
Code 4.3.2.1 Matlab code for determining the Elastic modulus.....	28

Chapter 1: Introduction

1.1 Background: Breast Cancer in Africa

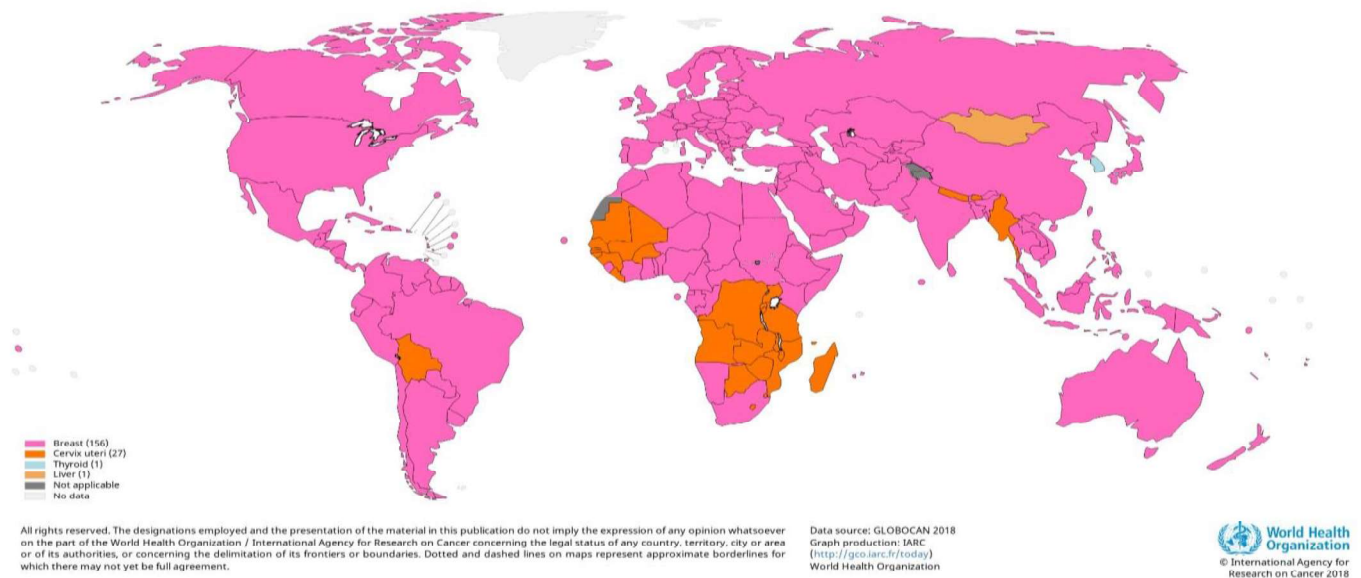


Fig 1.1 shows the heat regions for breast [pink], cervix [brown], and other cancers globally

Breast cancer is an abnormality that occurs when the breast cells begin to grow out of control. These cells divide more rapidly than healthy cells and continue to accumulate, forming a lump or mass. Breast cancer begins with cells in the milk-producing ducts [1] (ductal carcinoma), glandular tissue called lobules (lobular carcinoma), and in some cases, other cells within the breast. Cancer becomes invasive once it escapes the duct. Breast cancer is the top cancer in women in the developed and the developing world. Globally, about 25% and 15% of all new cancer cases and cancer deaths, respectively, among females were due to breast cancer [2]. Although little is said about this, men get affected by breast cancer as well. For men, the lifetime risk of being diagnosed with breast cancer is about 1 in 833.

The incidence of breast cancer increases in the developing world due to increasing life expectancy, increasing urbanization, and adopting Western lifestyles [2]. The majority of breast cancers develop in low- and middle-income countries where breast cancer is diagnosed at very

late stages. As shown in Fig 1.1, African countries face the double burden of cervical and breast cancer and need to implement combined cost-effective and affordable interventions to tackle these highly preventable diseases.

The socio-economic factors addressed when efforts are made to reduce the complications that arise from breast cancer are the 3rd goal of the Sustainable Development Goals: to promote good health and well-being [4] and the 5th Millennium Development Goals [5]: to improve maternal health. To the 5th MDG goal, research shows women are primarily in danger of breast cancer, and nursing and lactating mothers are at a higher risk. This is because the mother's health is affected, and it further affects the child's health as milk production declines.

1.2 Problem Definition

Early detection to improve breast cancer outcome and survival remains the cornerstone of breast cancer control [2]. Many initiatives have been taken to reduce late detection. Educating people through the media, campus visits, organizing workshops at workplaces, and free breast screening programs are a few of these initiatives. According to the American Cancer Society, when breast cancer is detected early and is in the localized stage, the 5-year relative survival rate is 99% [3]. Early detection is enhanced by conducting monthly breast self-exams and scheduling regular clinical breast exams and mammograms. The only breast cancer screening method that has proved to be effective is mammography screening [2] which is very costly, and therefore low-cost screening approaches, such as clinical breast examination, have been implemented. However, limited resources in a typical African country, especially in the rural or rural-urban backgrounds, have made it challenging to reduce the percentage of late-stage breast cancer detection.

1.3 Project Aims & Objectives

Many developments were made to promote the early detection of breast cancer. For instance, Mammography was proven to be effective in detecting cancer cells but was costly. As a result, Clinical Breast Examination (CBE) was implemented in limited-resource settings to help detect breast cancer [2]. There are many limitations from the previous screening technologies that can still be improved upon to promote early detection. The limitations are what informed the main aims and objectives of this project.

The objectives of this project are to develop a new breast screening product which is:

A. Portable and cost-effective. A less expensive device will encourage patronage because it will be affordable to the masses, increasing the number of people performing regular breast screening.

B. Easy to operate and requires little technical expertise. In this way, monthly breast examinations will be encouraged. Results obtained must also be easy to interpret without the help of a health professional.

C. Finally, they must be safe. After prolonged exposure to them, the existing methods can cause complicated health conditions or severe pain on the breast, as in Mammography and MRI. The new device must therefore be harmless to the user and safe for regular use.

Chapter 2: Literature Review

2.1 Breast Cancer Overview

There are many different types of breast cancer, and common ones include ductal carcinoma in situ (DCIS) and invasive carcinoma [6]. Others, like phyllodes tumors and angiosarcoma, are less common. Invasive ductal carcinoma (IDC), often referred to as infiltrating ductal carcinoma, is the most common type of breast cancer. About 80% of all breast cancers are invasive ductal carcinomas [7]. Invasive means that the cancer has “invaded” or spread to the surrounding breast tissues. Ductal means that the cancer began in the milk ducts, which are the “pipes” that carry milk from the milk-producing lobules to the nipple [7]. Carcinoma refers to any cancer that begins in the skin or other tissues that cover internal organs — such as breast tissue [7].

Altogether, ‘invasive ductal carcinoma’ refers to cancer that has broken through the wall of the milk duct and begun to invade the tissues of the breast. Over time, invasive ductal carcinoma can spread to the lymph nodes and possibly to other areas of the body. Figure 2.1 shows an image of the human breast showing the different regions where tumors grow.

Symptoms of Breast Cancer

Before one undertakes breast screening, some symptoms can provide foreknowledge on the possible presence of breast cancer. These symptoms include the change in shape & size of the breast, bloody nipple discharge, skin irritations such as puckering or dimpling, red rash, and pain in the breast [7]. These symptoms are summarized in figure 2.1

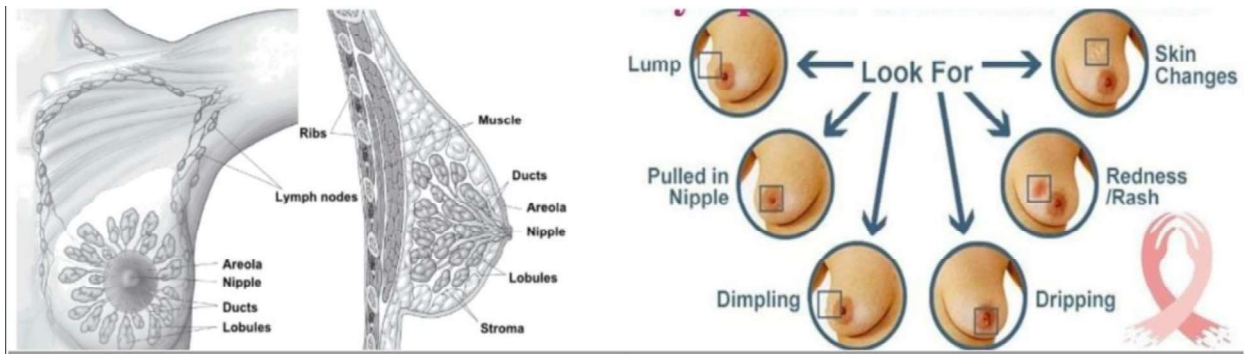


Figure 2.1.1.1 A labeled anatomy of the breast(left) and symptoms of breast cancer (right)

2.1.1 Breast Cancer Stages

Clinical staging is based on the results of tests done before surgery, which may include physical examinations, mammograms, ultrasound, and MRI scans. Pathological staging is based on what is found during surgery to remove breast tissue and lymph nodes. In general, pathological staging provides the most information to determine a patient's prognosis [8].

The five (5) stages of cancer are [8]:

- Stage 0: This stage describes cancer in situ, which means “in place.” Stage 0 cancers are still located in the place they started and have not spread to nearby tissues. This stage of cancer is often highly curable, usually by removing the entire tumor with surgery.
- Stage I: This stage is usually a small cancer or tumor that has not grown deeply into nearby tissues. It also has not spread to the lymph nodes or other parts of the body. It is often called early-stage cancer.

➤ Stage IA & Stage IB

- Stage II and Stage III: In general, these two stages indicate more significant cancers or tumors that have grown more deeply into nearby tissue. They may have also spread to lymph nodes but not to other parts of the body.

➤ Stage IIA, Stage IIB & Stage IIIA, Stage IIIB, Stage IIIC

- Stage IV: This stage means that the cancer has spread to other organs or parts of the body. It may also be called advanced or metastatic cancer.

This project will be focussing on detecting cancer cells when in stages 0 and 1 only. This is because the cancer cells are localized at these stages and have not grown into nearby tissues, hence, easy to detect. Detection at this stage is termed early-stage detection, which I aim to promote with this project.

2.2 Breast Cancer Imaging Procedures

In detecting the existence of a cancer cell and its stage, individuals undergo medical screening. Screening methods include: *Physical exams, laboratory tests via blood or urine samples, genetic tests, and imaging procedures [7]*. Imaging procedures are majorly used for diagnosing breast cancer. This method takes pictures of areas inside the body and is interpreted by medical doctors to diagnose breast cancer.

The imaging procedures that are conducted in detecting cancer cells in the breast include:

i. Ultrasonography (A of Fig 2.2.1) – Ultrasonography is a cost-effective and widely available screening tool, which detects tumors by bouncing acoustic waves off breast tissue [9]. The images produced are known as sonograms. Breast ultrasound is a non-invasive test. It is often used as a follow-up test after an abnormal finding on a mammogram, breast MRI or clinical breast exam. However, breast ultrasonography fails to detect many tumors because the acoustic properties of healthy and cancerous tissues are very similar [10].

ii. Mammography (B of Fig 2.2.1)-Mammography is the process of using low-dose X-rays, usually around 0.7 mSv (millisievert: a radiation dose measurement), to examine the human breast. A mammogram is simply performing an X-ray on the breast to detect cancerous cells. The technologist places the breast on a clear plastic plate while another plate will firmly press

the breast from above. The plates will flatten the breast, holding it still while the X-ray is being taken [11]. Mammography is the current standard breast screening technique, but it is less effective for subjects under 40 years old and dense breasts, less sensitive to small tumors (less than 1 mm, about 100,000 cells), and does not indicate eventual disease outcome [10].



Figure 2.1.1.1 shows the imaging techniques used in detecting cancer cells in the breast.

iii. Positron Emission Tomography/ Clinical Tomography (PET/CT) (C of Fig 2.2.1)-

Positron emission tomography (PET) scan uses a special dye containing radioactive tracers. These tracers are either swallowed, inhaled, or injected into a vein in your arm depending on what part of the body is being examined [12]. A computer then interprets the signals into images, which reveal biological maps of normal organ function and failure of an organ system [13]. A computerized tomography (CT) scan combines a series of X-ray images taken from different angles around your body and uses computer processing to create cross-sectional images. CT scan images provide more detailed information than plain X-rays do [14].

iv. Magnetic Resonance Imaging (MRI) (D of Fig 2.2.1)-MRI produces very clear pictures of the breast. MRI creates these images at different cross-sections by applying a strong magnetic field with RF signals [15]. Magnetic resonance imaging (MRI) can detect small lesions that cannot be detected by Mammography or ultrasound as it is more sensitive; however, it is also expensive and has low specificity, which can lead to overdiagnosis [16]. Breast MRI has been recommended for high breast cancer risk subjects, but it has not been recommended for the general population due to its high false-positive rate of 83%, high cost, and time consumption [17],[18].

v. Piezoelectric Finger (PEF) iBreast (E of Fig 2.2.1)-A handheld compression probe containing a 4×4 array of piezoelectric tactile pressure sensors which scans the breast and displays finding in real-time. PEF is a piezoelectric cantilever that consists of a top driving piezoelectric lead zirconate titanate (PZT) layer and a bottom sensing PZT layer between to a stainless-steel layer. CT, MRI, and ultrasound scans show the tissue density contrasts but provide no information on tissue stiffness. The PEF works with the principle of determining tissue stiffness to detect normal and abnormal tissues. [19]

MRI seems to have the highest sensitivity, while the CT scan has the highest specificity from the table shown below. Considering the time taken, the limitations, and the sensitivity and specificity values, the CT scan proves to be the best by far. However, the PEF probe seems to top the various imaging procedures in terms of cost and availability. From this conclusion, the piezoelectric method can be further improved to provide a cheaper but accurate screening procedure.

Table 2.1.1.1 Comparison of the existing breast cancer imaging procedures. [10,19,21]

Type	Use	Sensitivity (%)	Specificity (%)	Limitations	Time
Ultrasound	Evaluate lumps found in mammography, Not suitable for bony structures	83.0	34.0	Experienced operator is required during examination, low resolution image	10-20 mins
Mammography	Mass screening. Image bone, soft tissue and blood vessels all at the same. Shadowing due to dense tissues	67.8	75.0	Ionizing radiation, low sensitivity and specificity, sensitivity drops as tissue density increases	few seconds
PET	Functional imaging of biological processes. To image metastasis or response to therapy	61.0	80.0	Ionizing radiation, radioactive tracer injection	90-240 mins
CT	To determine and image distant metastasis in a single exam	91.0	93.0	Radiation risks, expensive scanner	5 mins
MRI	Young women with high risk; Images small details of soft tissues	94.4	26.4	Some types of cancers cannot be detected such as ductal and lobular carcinoma; expensive	40-60 mins
PEF	Monitoring changes of structural mechanical properties for real-time health detection.	93.0	90.0	Sensitive to small change in hand movement which introduces error.	30-40 mins

Chapter 3: System Requirements & Innovative Design

3.1 Hardware and Software Requirements

3.1.1 *Hardware Requirements:*

The hardware requirements involve the physical outlook of the system and the devices needed to build the system. These hardware requirements include:

1. **Ease of use and portability:** The system must be operated without needing much technical expertise and must be easily handled or transported to make it readily available. Existing breast scanning devices, such as MRI, require trained health workers to operate them. Personnel in lower-income areas are limited, and hence, the number of examinations that can be conducted are limited. In the long run, the probability of recording more early detection events is low.

2. **Cost-effective:** To address the high cost of services hindering individuals from obtaining clinical examinations, the device should be affordable so that breast examinations can be frequently done and carried out by a significant number of people.

3. **Sensitive and specific:** The system must have a high sensitivity and specificity of at least 85% and above to provide reliable information. Sensitivity, in medical terms, is a measure of how often a sensor/test can generate a true positive result for a condition, while specificity measures the ability to correctly generate a true negative result for a condition that is being tested [20].

4. **Safe:** Unlike other screening methods, the procedure in examining must not be harmful to the user.

3.1.2 *Software Requirements:*

1. **Wireless connectivity:** The system must transmit and store data wirelessly on any mobile device or computer for easy transfer and data access.

Wireless transmission is considered because:

- a. It is generally **cost-effective** as the capital for fixing cables, wires, and the general maintenance of the system is reduced when using wireless communication.
 - b. Since we aim to make our system portable, **mobility** is of great essence, and wireless networks grant the liberty to move around while devices remain connected over distances.
 - c. **High-speed data transmission.** Because a lot of data will be transmitted, having a high data transmission speed will increase the system's efficiency.
 - d. Wireless networks, although they encounter security issues such as signal interference and data corruption, they are more **reliable** as they do not include cables where harm could easily be done to them through ecological conditions such as rainfall.
2. **Fast translation and interpretation of data:** The system must be able to translate and interpret data into a form that can be used to diagnose the presence of a normal, malignant, or suspicious tissue in the breast. A microcontroller with high processing speed, a large memory for data storage, and the ability to convert data from the analog to digital form must be used to accomplish this task.

3.2 **System Design and Device Selection**

3.2.1 *System Design:*

The World Economic Forum's Global Competitiveness Index shows that out of 133 countries, Ghana ranks 112th on technological readiness [22]. However, to make this new

system adaptable, the traditional method of examining the breast will be inculcated in the system. The traditional method: clinical breast examination (CBE), involves using the pads of two fingers (thumb and pointer), as shown in figure 3.2.1.1, to examine the breast. The new system will have a biosensor placed on the tip of a glove to examine and read data more accurately rather than depending on the sensations of the fingers to detect lumps. Maintaining the old method of examination will make the system more adaptable, as it takes longer for local citizens to adapt to new technology. The inclusion of the biosensor will only be an innovation on the existing technology.

Studies have shown that breast cancers are stiffer than surrounding breast tissues. Increasingly, researchers have sought to detect breast tumors by means of tissue stiffness contrast by mechanical or optical means [19]. This detection method will also be employed in this project as it is relatively cheaper and easy to conduct. The response from the biosensor will be translated into elastic modulus values to determine a normal or malignant tissue. To accomplish this, the signal input from the sensor will be monitored on an oscilloscope to study the signal and perform necessary signal conditioning.

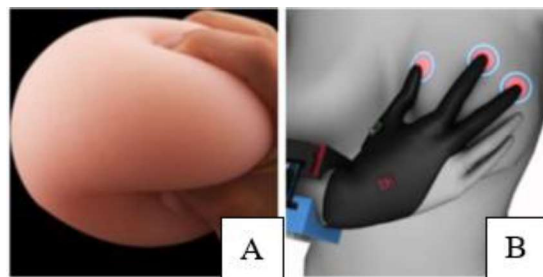


Figure 3.2.1.1 Method of examination (A) and how the system will be operated (B)

The output signals will then be converted to digital form (voltage) using an analog-digital converter. The voltage signals are converted into modulus of elasticity using :

$$E = \frac{1}{2} \left(\frac{\pi}{A} \right)^{\frac{1}{2}} (1 - v^2) \left[\frac{V_{in,0} - V_{in}}{V_{in}} \right] \text{ (Equation 3.2.1.1) [19]}$$

where A is the cross – sectional area of the sensor

v is the Poisson ratio of the tissue

$V_{in,0}$ is the induced voltage without the tissue

V_{in} is the induced voltage with the tissue

The elasticity values obtained from examining the breast will be compared to the approved elastic modulus of a normal and malignant tissue which are: 3-33kPa and 6-107kPa [19], to conclude whether a cancer cell has been detected. The data will be displayed on a screen by wirelessly transferring it to the displaying device such as a mobile phone or a computer.

Note: The information received after using the system can be shared with an oncologist to re-investigate and confirm the presence or absence of breast cancer cells or other possible complications. The system aims to promote the early detection of breast cancer. The best protection is early detection.

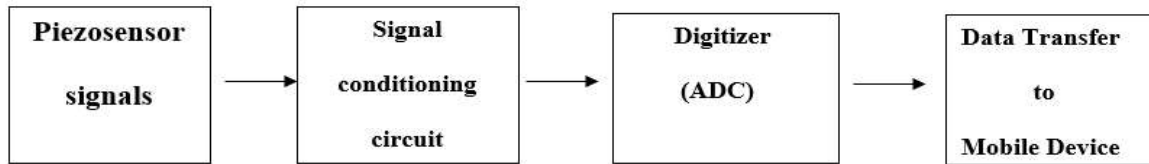


Figure 3.2.1.2 Block diagram of the proposed system

3.2.2 Device Selection

Biosensor selection: Biosensors can be classified according to the mode of physicochemical transduction or the type of biorecognition element. Based on the transducer that is employed for the detection and analysis of signals, biosensors can be classified as electrochemical, optical, thermal, and piezoelectric biosensors [23]. Under these biosensors, the primary transducers used for imaging purposes are ultrasound, infrared imaging (Digital

Infrared Thermal Imaging) [24], RF signals (MRI and X-ray for mammograms, CT, and PET scans).

Table 3.2.2.1 Pugh chart analyzing the major biosensors which can be used in detecting breast cancer cells.

Selection Criteria	Baseline	Ultrasound	RF signals	Piezoelectric	Infrared
Availability	0	+1	0	+1	+1
Cost effective	0	-1	-1	+1	-1
Portability	0	+1	0	+1	0
Specificity	0	+1	+1	+1	+1
Sensitivity	0	+1	+1	+1	+1
Safety	0	+1	0	+1	0
Total	0	+4	+1	+6	+2

As seen in the table, the piezoelectric sensor is the selected biosensor, majorly because of its availability, affordability, portability, and safety, which are key objectives needed to be met for the new system.

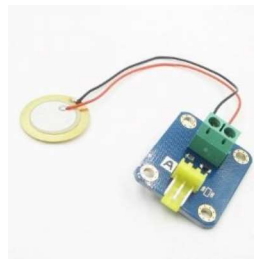


Figure 3.2.2.1 Analog Ceramic Piezo Vibration Sensor

Piezoelectric sensor: The piezoelectric material allows for converting energy from the mechanical domain to the electrical domain and vice versa [25]. The voltage induced from pressure is proportional to the applied pressure, and the piezo devices can be used to detect single pressure events and repetitive events. They are easily accessible and affordable. The analog ceramic piezo vibration sensor (3.3/5V) is a high-impedance device with a frequency of 28kHz and produces a small output signal [26]. The surface charge produced by an applied

force can be neutralized easily by the input resistance of other connected electronics. This makes the sensor behave as a high-pass filter for input signals, impeding pure static measurements[27]. Therefore, using a low-pass filter for signal conditioning can be implemented before interfacing with a data acquisition system.

Low-pass filter: To ensure accurate reading of signals, the high-frequency noise in the signal must be removed. A low-pass filter is connected in series to the input signal coming from the analog device to allow the passage of frequencies to 40Hz [26]. A low-pass filter with a threshold of 40Hz can be achieved based on the calculation presented in Equation 3.2.2.1:

given $f_c = 40\text{Hz}$, where $f_c = \text{cutoff frequency}$, $R = \text{resistance}$ & $C = \text{capacitance}$.

$$f_c = \frac{1}{2\pi RC} \quad (\text{Equation 3.2.2.1})$$

Three $1\mu\text{F}$ in series = $0.33\mu\text{F}$.

$$R = \frac{1}{2\pi * 40 * 0.33\mu\text{F}} = 12\text{k}\Omega$$

Finding R , we obtain $12\text{k}\Omega$ which can be achieved using a $10\text{k}\Omega$ and $2\text{k}\Omega$ in series.

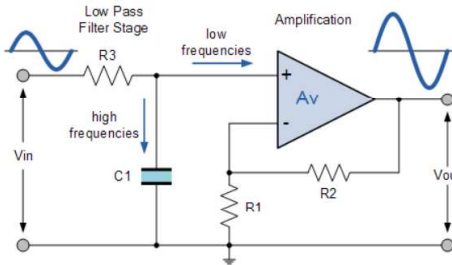


Figure 3.2.2.2 is the active low-pass filter with a gain arrangement for amplification

Operational amplifier: The low-frequency signals allowed in from the sensor can be amplified to a sufficient amplitude before further processing. A non-inverting amplifier is used because the output generated is in phase with the applied input, unlike in the inverting amplifier where the input and output signals generated are within a 180 degrees phase shift.

The UA741-N is selected as the OpAmp to its large input voltage range, high gain, and short-circuit protection [28].

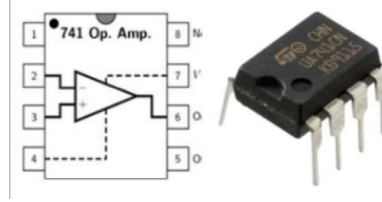


Figure 3.2.2.3 The UA741-N operational amplifier

For testing, the non-inverting OpAmp will be designed to develop a gain of 5. To achieve this, see Equation 3.2.2.2:

$$\text{Available resistor} = 1k\Omega$$

$$\text{Gain} = 1 + \frac{R2}{R1} \quad (\text{Equation 3.2.2.2})$$

Assuming a gain of 5;

$$5R1 = R1 + R2$$

$$R2 = 4k\Omega$$

To simplify the circuit, a $4.7k\Omega$ was used for R2; hence the gain obtained was 5.7.

Micro-processor & Development Board: The ARM® Cortex™-M0+ processor on the FRDM KL25Z board will be used to process and analyze the signal received. This processor is a configurable, multistage, 32-bit RISC (Reduced Instruction Set-Computing) processor [29]. It has a memory protection functionality and can conduct interrupt handling to prioritize tasks [29]. The processor was selected due to its high processing speed, low cost, energy efficiency, and, mainly, its availability. An analog to digital conversion will be implemented using the FRDM KL25Z to convert the analog signal to voltage values analyzed using the modulus of elasticity formula (Equation 3.2.1.1) to determine if readings show a normal or malignant tissue.

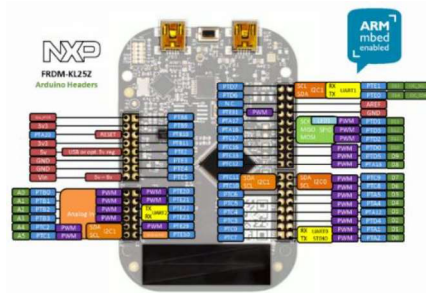


Figure 3.2.2.4 NXP FRDM KL25Z Board

Data communication device: In deciding which wireless technology will be best in transferring the data, a few criteria were selected to compare the common wireless technologies [30],[31]. As seen in Table 3.2, the Bluetooth module (HC-05) was selected to be the most appropriate for this project due to its availability and low power consumption.

Table 3.2.2.2 Pugh chart showing Bluetooth (figure 3.2.2.5) as the most appropriate option for the project

Wireless Technology Pugh Chart

Selection criteria	Wi-Fi	Bluetooth	Infrared communication	NFC (Near Field Communication)
Cost effective	2	2	1	1
Speed	2	2	2	1
Coverage	2	2	2	1
Security	1	1	1	2
Availability	2	2	1	2
Size	0	2	1	2
Power consumption	0	2	1	2
Total	9	13	9	11

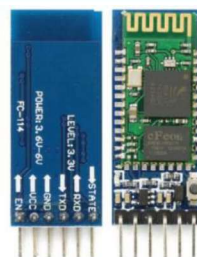


Figure 3.2.2.5 Bluetooth module (HC-05)

Chapter 4: Implementation, Testing & Results

4.1 Modeling of the Breast and Tumor Phantoms

From literature [19], breast and tumor phantoms were made to depict the actual human tissues. The concentration of the breast phantom was 0.10g/ml, with an elastic modulus (E) similar to that of normal breast tissues, about 10 kPa [19]. The phantom was modeled using gelatin. The three (3) breast phantoms contain four (4) tumor phantoms each (figure 4.1), modeled using modeling dough.

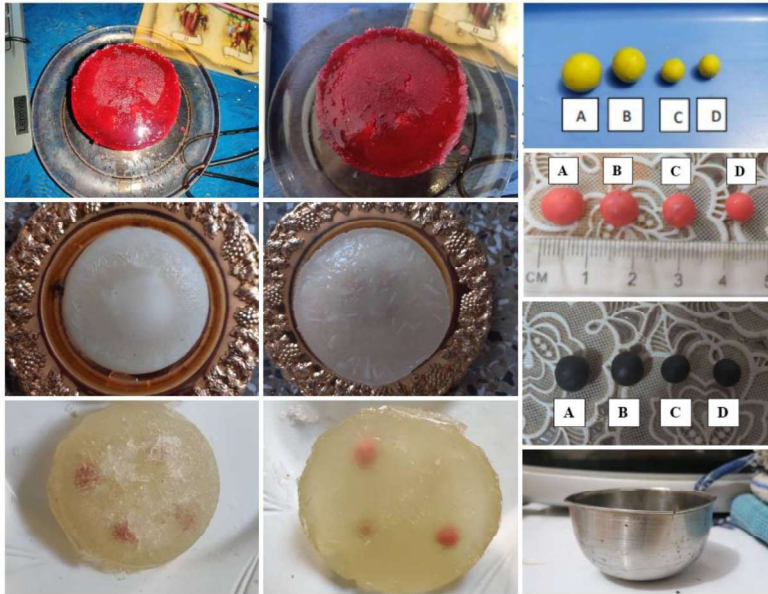


Figure 4.1 shows the three breast phantoms, the tumor phantoms, and the mold used for modeling the breast phantoms.

4.1.1 Methodology and Measurements

Breast phantom: Pour powdered gelatin (about 85g) or place nine leaf gelatins (17g) in cold water and stir till it blooms. While in the mold, allow the gelatin to dissolve in hot water. The process can be quickened by stirring the gelatin. Refrigerate for approximately 4 hours. The mass of the gelatin product and the volume of the water (approximated by the

volume of the mold used) were used to compute the concentration of the breast phantom. The volume of the mold was determined by computing the volume of a hemisphere (Equation 4.1.1.).

$$\text{Concentration} = \frac{\text{Mass}}{\text{Volume}} \quad (\text{Equation 4.1.1. 1})$$

$$\text{Volume of hemisphere} = \frac{2}{3}\pi r^3 \quad (\text{Equation 4.1.1. 2})$$

Table 4.1.1.1 Concentration of breast phantoms. The masses of the gelatin product used and the volume of the mold were used in this computation.

Phantom	Diameter (cm)	Mass(g)	Vol (ml)	Concentration (g/ml)
A	9.00	85	190.852	0.445
B	9.00	19	190.852	0.089
C	9.00	19	190.852	0.089

Tumor phantom: The tumor phantoms were created using modeling clay. The modeled phantoms measured:

Table 4.1.1.2 Measurement of three sets of tumor phantoms

Phantom	Actual diameter (from literature) [19]	Diameter (mm)	Diameter (mm)	Diameter (mm)
A	11.50 ±0.30	11.50 ±0.30	11.40 ±0.30	11.10 ±0.30
B	10.30 ±0.30	10.00 ±0.30	10.00 ±0.30	10.20 ±0.30
C	7.80 ±0.20	8.00 ±0.20	7.90 ±0.20	8.10 ±0.20
D	6.20 ±0.20	6.30 ±0.20	6.00 ±0.20	6.10 ±0.20

4.2 Implementation

The hand-gloves are made of high-quality cotton, which can easily stretch. The glove fits the hands without a cumbersome feeling, and it is therefore comfortable to use. The piezo sensors connected to the breadboard are attached to the tips of the hand glove using duct tape.

A breadboard power supply is used to power the prototype, which enables easy movement without wire interferences.

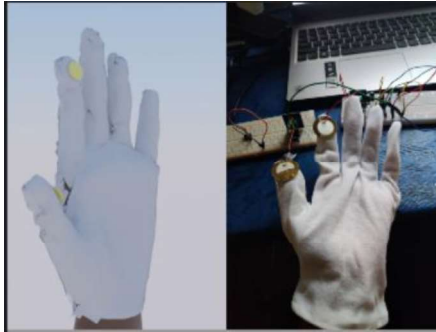


Figure 4.1.1.1 3D modeled system using Blender app (left) and real-life system(right).

4.2.1 Schematic Diagram and Breadboard Representation of the Circuit.

The circuit diagrams (Figure 4.2.1.1) were created using Fritzing software. The breadboard and schematic diagram were manually set up using the devices selected and informed calculations made in section 3.2.2.

Description of circuit: A breadboard power supply will be used to deliver 5V to the entire circuit. All the components used require 3.3/5V and so the voltage being delivered is safe for the system. The piezo sensor is connected in parallel to a low-pass filter having a cut-off frequency of 40Hz. The signals are then fed into the non-inverting amplifier for amplification of gain; **5.7**. The analog signal is fed into the FRDM KL25Z development board and converted to digital form using an analog-to-digital conversion (ADC) code (4.1) deployed using the Keil Uvision software. The Bluetooth connection between the development board and the mobile device is set up using a serial universal asynchronous receiver-transmitter (UART) code (4.2). As shown in figure (next), the data from the sensor is being read as voltage values on the mobile device via Bluetooth transfer. The Serial Bluetooth terminal on the phone serves as an interface between the phone and the development board where the values will be displayed.

Another task the algorithm performs is to light different LEDs based on the conclusion drawn from the data analysis. A **red** light shows on the FRDM board if a tumor has been identified. A **yellow** light shows when the nature of the tissue is uncertain. A reading is uncertain if the sensor records an abnormality which may not necessarily be breast cancer. A **green** light appears if no tumor is detected, this means the voltage reading represents a normal tissue. The code snippet 4.2.3 shows the algorithm that will perform this task.

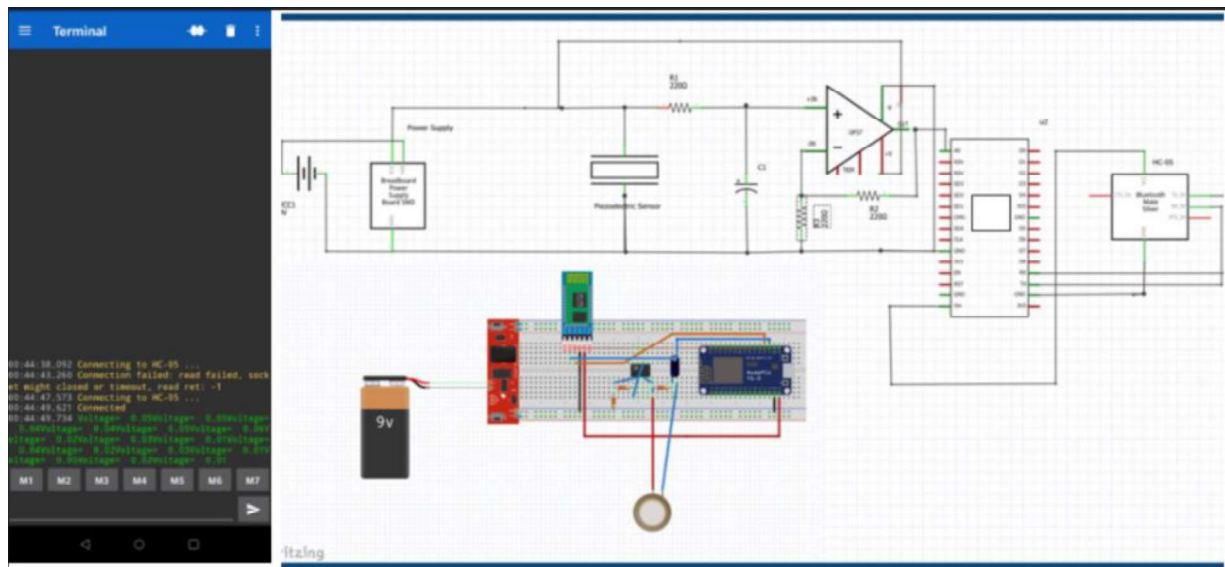


Figure 4.2.1.1 Bluetooth terminal displaying voltage readings (left) and the schematic diagram & breadboard representation of the system.

Code 4.2.1.1 Code snippet performing ADC

```
#include "MKL25Z4.h"
void init_ADC (void) {
SIM->SCGC6 |= SIM_SCGC6_ADC0_MASK; //clock gating ADC0
SIM->SCGC5 |= SIM_SCGC5_PORTE_MASK; //clock gating port E
PORTE->PCR[PTE20] &= ~PORT_PCR_MUX_MASK; // Select analog for pin
PORTE->PCR[PTE20] |= PORT_PCR_MUX (0);
// use low power and long sample time to improve accuracy
ADC0->CFG1=ADC_CFG1_ADLPSC_MASK|ADC_CFG1_ADLSMP_MASK; //select
channel 1 as input
ADC0->CFG1 |= ADC_CFG1_MODE (3); //MODE:16 bit single-ended
conversion when DIFF=0
ADC0->SC2 = ADC_SC2_REFSEL (0); //reference voltage
}
// taking avg of 32 samples ((2^2) ^N, N=3
float measure_POT (void) {
```

```

float val;
unsigned int sample =0;
ADC0->SC1[0] = 0x00; // start conversion on channel 0
while (!(ADC0->SC1[0] & ADC_SC1_COCO_MASK)); //conversion complete
sample = ADC0->R[0]; //has the result of an ADC conversion
val = (float)5*sample/0xffff;//0xffff maps to max of 5v
return val;
}

```

Code 4.2.1.2 Code snippet setting up serial Bluetooth connection

```

void Init_UART(void){
//select clock for uart0 (disabled by default), MCGFLLCLK/system
clk as UART0 clock
SIM->SOPT2 |= SIM_SOPT2_UART0SRC(1);
// clock gate UART0
SIM->SCGC4 |= SIM_SCGC4_UART0_MASK; //clock gate UART0
//compute set baud rate (SBR), choosing baud rate of 9600 for BT
uint8_t sbr = (uint16_t)((SYS_CLOCK)/((OSR+1) *BAUD_RATE));
//default OSR is 15, sbr=136.5, SYS_CLOCK =20971520u
//UART0->BDH |=((sbr>>8) & 0x1F); //generic. set only bottom 5
bits
UART0->BDH =0; //0x0 for this calculation
UART0->BDL=sbr; //0x88 for this calculation
// Rx Interrupt,Tx & RX enable
UART0->C2 |= UART_C2_RIE_MASK | UART_C2_TE_MASK | UART_C2_RE_MASK;

NVIC_SetPriority(UART0_IRQn, 3);
NVIC_ClearPendingIRQ(UART0_IRQn);
NVIC_EnableIRQ(UART0_IRQn);

void UART0_IRQHandler(void) {
uint8_t ch;
if (UART0->S1&(UART_S1_OR_MASK|UART_S1_NF_MASK|UART_S1_FE_MASK|
UART_S1_PF_MASK)){ // clear the error flags
UART0->S1 |= UART0_S1_OR_MASK|UART0_S1_NF_MASK|UART0_S1_FE_MASK|
UART0_S1_PF_MASK; // read the data
register to clear RDRF
ch = UART0->D;
}
if (UART0->S1 & UART0_S1_RDRF_MASK) { //received character or
wholeval
ch = UART0->D;
rxChar=ch; //whole=ch;
lightLED(); //turn on LED based on value recorded
if (!Q_Full(&RxQ)) {
Q_Enqueue(&RxQ,ch);
} else {
}}
}

```

```

    if((UART0->C2&UART0_C2_TIE_MASK)&&(UART0->S1
&UART0_S1_TDRE_MASK)){ //transmitter interrupt enabled & tx buffer
empty
    if (!Q_Empty(&TxQ)) { //can send another character
        UART0->D = Q_Dequeue(&TxQ);
    } else {
        // queue is empty so disable transmitter interrupt
        UART0->C2 &= ~UART0_C2_TIE_MASK;
    }}

```

Code 4.2.1.3 On-board LED setup and Control

```

#define RED_LED_POS (18)           // on port B
#define GREEN_LED_POS (19) // on port B
#define BLUE_LED_POS (1)          // on port D
#define malignantTisVal 1.5
#define normalTisVal 1
#define uncertainTisVal 0.5
//led setup and control
void Init_RGB_LEDs(void) {
    // Enable clock to ports B and D
    SIM->SCGC5 |= SIM_SCGC5_PORTB_MASK | SIM_SCGC5_PORTD_MASK;
// Make 3 pins GPIO
    PORTB->PCR[RED_LED_POS] &= ~PORT_PCR_MUX_MASK;
    PORTB->PCR[RED_LED_POS] |= PORT_PCR_MUX(1);
    PORTB->PCR[GREEN_LED_POS] &= ~PORT_PCR_MUX_MASK;
    PORTB->PCR[GREEN_LED_POS] |= PORT_PCR_MUX(1);
    PORTD->PCR[BLUE_LED_POS] &= ~PORT_PCR_MUX_MASK;
    PORTD->PCR[BLUE_LED_POS] |= PORT_PCR_MUX(1);
// Set ports to outputs
    PTB->PDDR |= MASK(RED_LED_POS) | MASK(GREEN_LED_POS);
    PTD->PDDR |= MASK(BLUE_LED_POS);
//setting them off initially
    PTB->PSOR = MASK(RED_LED_POS);
    PTB->PSOR = MASK(GREEN_LED_POS);
    PTD->PSOR = MASK(BLUE_LED_POS);
}
void Control_RGB_LEDs(unsigned int red_on, unsigned int green_on,
unsigned int blue_on) {
    if (red_on) {
        PTB->PCOR = MASK(RED_LED_POS);
    } else {
        PTB->PSOR = MASK(RED_LED_POS);
    }
    if (green_on) {
        PTB->PCOR = MASK(GREEN_LED_POS);
    } else {
        PTB->PSOR = MASK(GREEN_LED_POS);
    }
    if (blue_on) {
        PTD->PCOR = MASK(BLUE_LED_POS);
    } else {

```

```

        PTD->PSOR = MASK(BLUE_LED_POS);
    }}void lightLED(void){
        if (whole<=malignantTisVal) {
            Control_RGB_LEDs(1,0,0);    //malignantTisVal
        }
        if (whole==normalTisVal) {
            Control_RGB_LEDs(0,1,0);    //normalTisVal
        }
        if (whole==uncertainTisVal) {
            Control_RGB_LEDs(0,0,1);    //uncertain TisVal
        }
    }}

```

4.3 Testing & Recording:

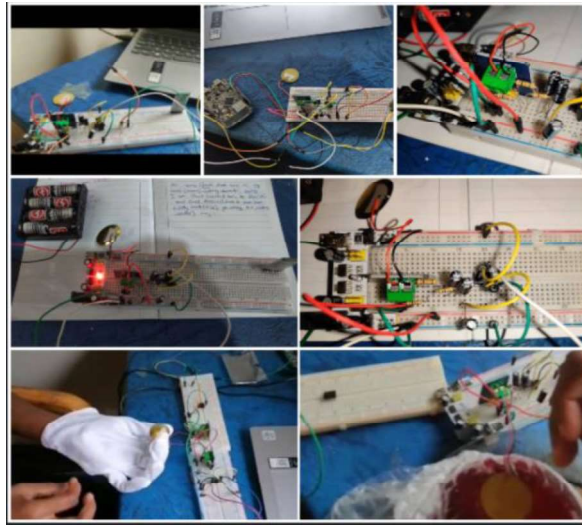


Figure 4.2.1 Final setup for testing and analysis

4.3.1 Amplification and Filtering test:

After setting up the circuit and with the phantoms ready, the first test was an amplification test to verify that the signals were being amplified accurately. To do this, I generated a sine wave using the Wavegen module in the Waveforms software with a frequency of 1kHz. The output signal obtained from the amplifier had an amplitude of 2V when it was initially 0.5 V. The same test was conducted using the piezo signal as input. A 0.5V signal was also amplified to a 2V signal. In conclusion, the signal was amplified by a gain of 4. The test outputs are displayed in Figure 4.3.1 A and B.

For the filtering test, a Wavegen signal having the same frequency as the piezo sensor: 28kHz, was fed into the low pass filter circuit. The low pass filter removed the noise and high frequencies that were captured from the input signal. The 28kHz signal produced an unstable waveform. After passing through the low pass filter, it moved to a frequency of 50Hz with an amplitude of 0.5 V (Figure 4.3.1 C). Figure 4.3.1 D shows the initial and final signals recorded when the Piezosensor was used. The yellow signal represents the initial signal, and the blue signal represents the final output signal.

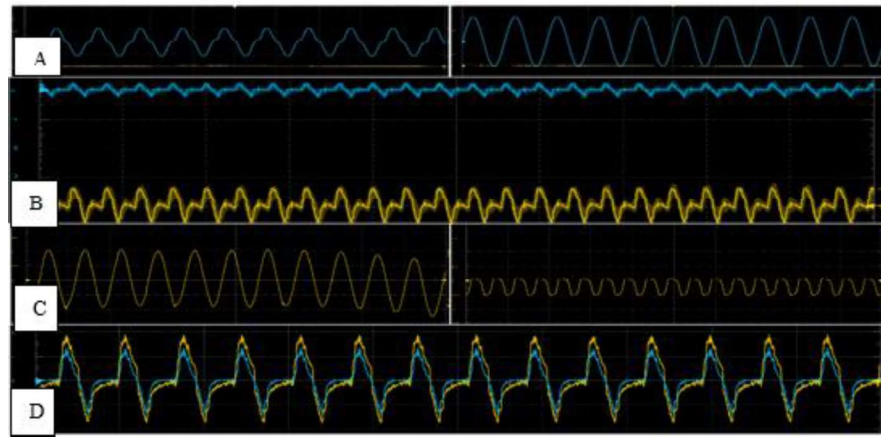


Figure 4.3.1 Amplification test (A/B), filtering test(C), and the signal output from piezo sensors after performing both tests(D).

4.3.2 Piezo sensor test without tissue phantoms:

This test was performed to monitor the output from the piezo sensor at rest. The values obtained from this experiment are the induced voltages without the tissue phantoms, which pass as $V_{in,0}$ for Equation 4.3.2.1. In this test, the yellow signal is from sensor 1, and the blue from sensor 2. Also, the thumb produced an offset of 0.1773 on sensor 1. 8000 data samples were obtained from each test.

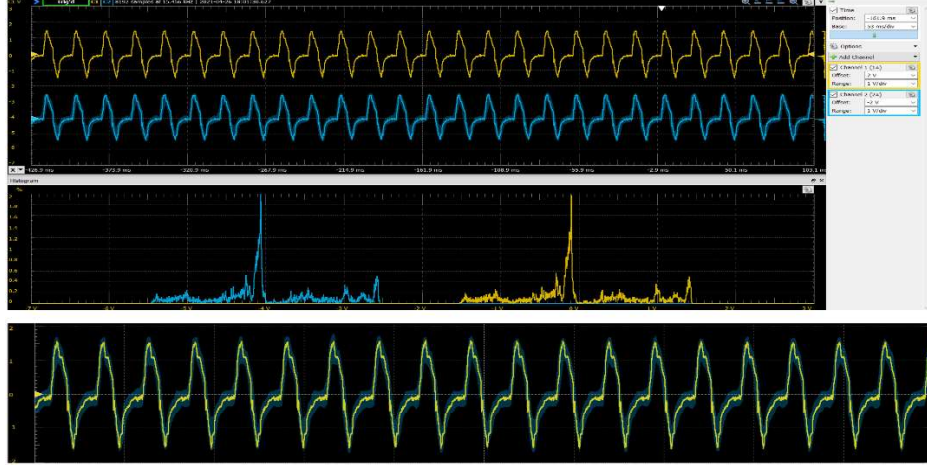


Figure 4.3.2.2 Piezo sensor test without the tissue phantoms.

Piezo sensor test with breast phantoms only:

This test was performed to monitor the output from the piezo sensor when placed on the breast phantom only. The values obtained from this experiment are the induced voltages which pass as V_{in} in Equation 4.3.2.2 for evaluating the Elastic modulus of the breast phantom without tumor. In this test, the yellow signal is from sensor 1, and the blue from sensor 2. It is expected that the values obtained in this test correspond to the Elastic modulus value of normal breast tissues, which range from 3-33kPa. The values obtained from the test are also monitored on a mobile device to ensure it correlates with the data from the oscilloscope. *See figure 4.3.2.1 for sample signal output from this test.*

Piezo sensor test with breast and tissue phantoms:

This test was performed to monitor the output from the piezo sensor when applied on the breast phantom containing tumors. The values obtained from this experiment are the induced voltages which pass as V_{in} in Equation 4.3.2.3 for evaluating the Elastic modulus of the breast phantom with tumors. In this test, the yellow signal shows sensor 1 readings, and the blue shows readings from sensor 2. *See figure 4.3.2.2 for sample signal output from this test.*

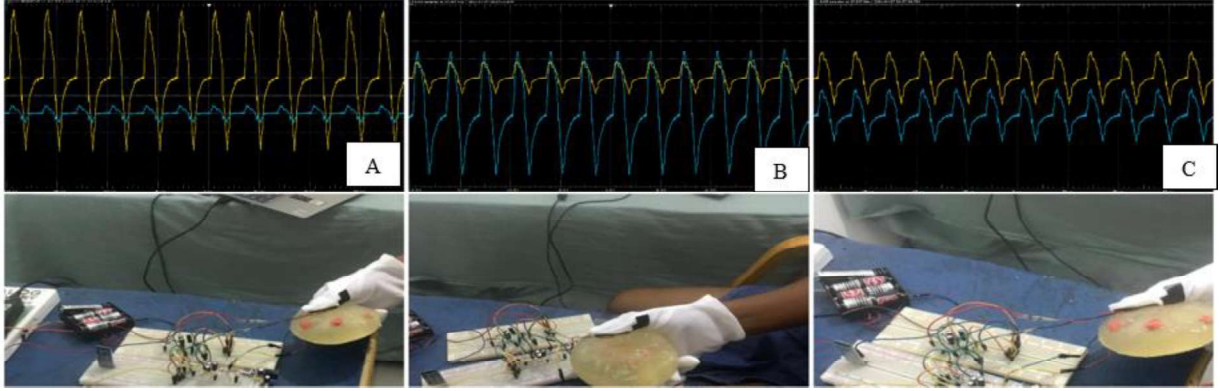


Figure 4.3.2.3 This figure shows a sample of signals produced when sensor 1 only(A), sensor 2 only(2) and both sensors are used to examine the different breast phantoms with and without tumors.

Chapter 5: Results & Discussions

5.1 Results & Discussions

The data from testing were extracted from Waveforms into Matlab to compute the Elasticity values using Equation 3.2.1.1. The Matlab code used is displayed in code 5.1 below.

$$E = \frac{1}{2} \left(\frac{\pi}{A} \right)^{\frac{1}{2}} (1 - \nu^2) \left[\frac{V_{in,0} - V_{in}}{V_{in}} \right]$$

where A is the cross-sectional area of the tissue :

$$\text{diameter of sensor} = 2.7\text{cm}, \text{area} = \frac{\pi d^2}{4} = 5.726\text{cm}^2$$

$V_{in,0}$ is the induced voltage without the tissue

V_{in} is the induced voltage with the tissue (breast only and breast & tumor)

ν is the poisson ratio of the tissue:

ν of modelling clay = 0.434-0.50 [32]

$$\text{average} = \frac{0.50 + 0.434}{2} = 0.467$$

ν of gelatin = 0.50 [33]

$$\nu \text{ is therefore } \frac{0.50 + 0.467}{2} = 0.4835$$

Since sensor 1 and 2 were used to examine the phantom from top and bottom respectively. The average of the sensor values obtained were used as V_{in} in computing the Elastic modulus for the different tests.

```
load('Krissy.mat')
```

```

area=5.726;%constant
pr=0.4835; %constant
Vino=Vino;
Vin=Vin_bo_p1;
time=t;
ElasticMod=(1/2) ((pi/area)^1/2) (1-(pr^2)) * ((Vino-
Vin)/(Vin));%equation to determine modulus of elasticity
plot(time,Vin, '-')
hold on
title('Vin against time')
xlabel('Time')
ylabel('Vin')

figure(2)
plot(Vin,ElasticMod, '-')
hold on
title('E against Vin')
xlabel('Modulus of Elasticity')
ylabel('Vin')

```

Code 4.3.2.1 Matlab code for determining the Elastic modulus.

Breast phantom 1 only

Images...Appendix for val

Breast phantom 1 with tumor

Breast phantom 2 only

Breast phantom 2 with tumor

The results were able to tell when a tumor was present in the breast phantom. The elastic modulus obtained for the tumor regions were as follows: tallying with the elastic modulus of a malignant tissue.

(put results here)

The values were further analyzed to determine the sensitivity and specificity of the system using the following equations:

$$\text{Sensitivity} = \frac{A}{A+C}, \text{ Equation 4.3.2.1 [34]}$$

$$\text{Specificity} = \frac{D}{D+B}, \text{ Equation 4.3.2.2 [34]}$$

Table 4.3.2.1 Case Definition [34]

	+	-	
+	A True Positives (10)	B False Positives(2)	Specificity=83.3%
-	C False Negatives (2)	D True Negatives(11)	Sensitivity=84.6%

Chapter 6: Conclusion

The limitations and challenges faced while researching and working on this project, including future works, will be discussed further in this chapter.

6.1 Conclusion

In creating a low-cost breast scanner detector, a piezoelectric sensor was used as a finger-tip sensor on a hand glove for screening. This is done by recording the varying voltages that the piezo records when placed on an object or vice versa. By applying the traditional method of breast self-examination, the sensor can report the presence or absence of a tumor. The KL25Z development board was used to deploy the algorithm for controlling the device.

After performing three tests on the three breast phantoms, the sensitivity and specificity of the system showed that the Piezo Breast Cancer Detector has relatively better values as compared to the existing methods. The information obtained from this device is therefore reliable and, as a start, can be used as a pre-screening device for early-stage breast cancer. In Africa, where many oncologists and breast cancer screening equipment are scarce, this device can be an excellent screening tool.

6.2 Challenges & Limitations.

One major challenge faced during this project is the COVID-19 pandemic. The pandemic contributed to some delays in purchasing and shipping components. It was a personal challenge moving around during the pandemic, and since the primary component, this is the piezoelectric sensor, was not available locally, it had to be purchased and shipped from overseas, which took approximately three weeks to arrive. This delayed the testing phase of my project. Another limitation the pandemic created was easy access to the instruments and components in the school laboratory. For example, it was hard estimating the mass of the breast phantoms, which would have assisted me in computing the densities of the breast phantom. Also, in attaching the sensor to the gloves, a glue gun would have been of great use, but the inability to obtain one meant I had to make do with a duct tape.

Financial constraints made the acquisition of some components and materials difficult, and this limited the number of materials used for the project, limiting the number of tests that could have been performed. *See bill of materials in Appendix D.*

There was a challenge displaying the different LED colors when a particular tissue was identified (normal, malignant, or uncertain) as the values were obtained were continuous and

were recorded rapidly. I used a Systick Handler to control the number of values recorded, but the issue was not fully resolved.

6.3 Future Work & Recommendations

In the future, I would display a map of the breast on the mobile or laptop device and show the exact location where the tumor was detected. The map can then be saved as an image and shared with an oncologist for further review and testing. Also, I will address the proper assembling of the sensors and the glove. A small open-pad structure could be made at the tips of the gloves where the sensors can be fixed and fastened. This will help stabilize the sensors and prevent errors while recording. The wires and microcontroller will be harnessed and placed in a pouch fixed behind the glove or worn on the wrist. *See figure below.*



Figure 4.3.2.1 Open-pad structure, circuit kept at the back of the hand or worn on the wrist.

Finally, I would recommend that more education on the early detection of breast cancer takes place on social media as it is the main source of information for this generation. Once the awareness is created, the number of deaths caused by breast cancer will reduce.

Also, it will be helpful if more research on this topic is conducted and funded to provide more cost-effective screening facilities for low and middle-income-earning countries.

REFERENCES

- [1] “What is breast cancer?,” Prevea. Available: <https://www.prevea.com/For-Patients/Your-Wellness/Resources/what-is-breast-cancer>.
- [2] “Breast cancer: prevention and control,” World Health Organization, 21-Jan-2016. Available: <https://www.who.int/cancer/detection/breastcancer/en/>.
- [3] “Breast Cancer Early Detection,” National Breast Cancer Foundation. Available: <https://www.nationalbreastcancer.org/early-detection-of-breast-cancer/>.
- [4] “Sustainable Development Goal 3: Health,” World Health Organization, 13-Jan-2016. Available: <https://www.who.int/topics/sustainable-development-goals/targets/en/#:~:text=SDG%203%20%E2%80%9CEnsure%20healthy%20lives,for%20all%20at%20all%20ages%E2%80%9D>.
- [5] “Millennium Development Goals,” UNDP. Available: https://www.undp.org/content/undp/en/home/sdgoverview/mdg_goals.html.
- [6] “Types of Breast Cancer: Common, Rare and More Varieties,” Cancer Treatment Centers of America, 12-Mar-2021. Available: <https://www.cancercenter.com/cancer-types/breast-cancer/types>.
- [7] “Invasive Ductal Carcinoma: Diagnosis, Treatment, and More,” 21-Jan-2020. Available: <https://www.breastcancer.org/symptoms/types/idc>.
- [8] “Stages of Cancer,” Cancer.Net, 14-Aug-2020. Available: <https://www.cancer.net/navigating-cancer-care/diagnosing-cancer/stages-cancer>.
- [9] D. C. Appleton, L. Hackney, and S. Narayanan, “Ultrasonography alone for diagnosis of breast cancer in women under 40,” Annals of the Royal College of Surgeons of England, Apr-2014. Available: <https://www.ncbi.nlm.nih.gov/pmc/articles/PMC4474049/>.

- [10] L. Wang, “Early Diagnosis of Breast Cancer,” Sensors (Basel, Switzerland), 05-Jul-2017. Available: <https://www.ncbi.nlm.nih.gov/pmc/articles/PMC5539491/>.
- [11] “What Is a Mammogram?” Centers for Disease Control and Prevention, 14-Sep-2020. Available: https://www.cdc.gov/cancer/breast/basic_info/mammograms.htm
- [12] “PET/CT Scans,” Lincoln, NE: Advanced Medical Imaging. Available: <https://amimaging.com/imaging-services/petct-scan/>.
- [13] B. Brian, “What Is A PET Scan?”, Healthline, 17-Sep-2018. Available: [https://www.healthline.com/health/petscan#:~:text=A%20positron%20emission%20tomography%20\(PET,the%20body%20is%20being%20examined.](https://www.healthline.com/health/petscan#:~:text=A%20positron%20emission%20tomography%20(PET,the%20body%20is%20being%20examined.)
- [14] “CT scan,” Mayo Clinic, 28-Feb-2020. Available: [https://www.mayoclinic.org/tests-procedures/ct-scan/about/pac-20393675#:~:text=A%20computerized%20tomography%20\(CT\)%20scan,than%20plain%20X%20Drays%20do.](https://www.mayoclinic.org/tests-procedures/ct-scan/about/pac-20393675#:~:text=A%20computerized%20tomography%20(CT)%20scan,than%20plain%20X%20Drays%20do.)
- [15] A. Berger, “Magnetic resonance imaging,” BMJ (Clinical research ed.), 05-Jan-2002. Available: <https://www.ncbi.nlm.nih.gov/pmc/articles/PMC1121941/>.
- [16] R. M. Mann, C. K. Kuhl, and L. Moy, “Contrast-enhanced MRI for breast cancer screening,” Journal of magnetic resonance imaging: JMRI, Aug-2019. Available: <https://www.ncbi.nlm.nih.gov/pmc/articles/PMC6767440/>.
- [17] “Magnetic Resonance Imaging,” Magnetic Resonance Imaging - an overview | ScienceDirect Topics. Available: <https://www.sciencedirect.com/topics/neuroscience/magnetic-resonance-imaging.>

- [18] N. Hoogerbrugge, Y.J.L. Kamm, et. al, “The impact of a false-positive MRI on the choice for mastectomy in BRCA mutation carriers is limited,” *Annals of Oncology*. Available: [https://www.annalsofoncology.org/article/S0923-7534\(19\)41446-4/fulltext](https://www.annalsofoncology.org/article/S0923-7534(19)41446-4/fulltext).
- [19] X. Xu, Y. Chung, A. D. Brooks, W.-H. Shih, and W. Y. Shih, “Development of array piezoelectric fingers towards in vivo breast tumor detection,” *NASA/ADS*. Available: <https://ui.adsabs.harvard.edu/abs/2016RScI...87l4301X/abstract>.
- [20] “Understanding medical tests: sensitivity, specificity, and positive predictive value,” *HealthNewsReview.org*. Available: <https://www.healthnewsreview.org/toolkit/tips-for-understanding-studies/understanding-medical-tests-sensitivity-specificity-and-positive-predictive-value/>.
- [21] “Advantages and disadvantages of piezoelectric sensor and its application,” *Advantages and disadvantages of piezoelectric sensor and its application-Industry news-weige Design studio Official-*. Available: http://pisuko.com/?list_30%2F113.html.
- [22] “Science, Technology & Innovation Policy Review - UNCTAD.” Available: https://unctad.org/en/docs/dtlstict20098_en.pdf.
- [23] “Biosensors,” *Biosensors - an overview | ScienceDirect Topics*. [Online]. Available: <https://www.sciencedirect.com/topics/engineering/biosensors>.
- [24] “Imaging and a Deep Learning Model.” [Online]. Available: http://eprints.utm.my/id/eprint/86379/1/AliSelamat2018_BreastCancerDetectionUsingInfrared.pdf.
- [25] “What is Piezoelectricity?,” *OnScale*. Available: <https://onscale.com/piezoelectricity/what-is-piezoelectricity/>.
- [26] S. K. Khandai and S. K. Jain, “Comparison of sensors performance for the development of wrist pulse acquisition system,” *TENCON 2017 - 2017 IEEE Region 10 Conference, 2017*, pp. 2870-2875, doi: 10.1109/TENCON.2017.8228351.
- [27] “Piezoelectric Sensor,” *Piezoelectric Sensor - an overview | ScienceDirect Topics*. Available: <https://www.sciencedirect.com/topics/engineering/piezoelectric-sensor>.

- [28] “UA741,” *STMicroelectronics*. Available: <https://www.st.com/en/amplifiers-and-comparators/ua741.html#:~:text=The%20UA741%20is%20a%20high%20performance%20monolithic%20operational,in%20integrators%2C%20summing%20amplifiers%20and%20general%20feedback%20applications>.
- [29] “FRDM-KL25Z,” *Mbed*. [Online]. Available: <https://os.mbed.com/platforms/KL25Z/>.
- [30] “Comparison of Wireless Technologies: Bluetooth, WiFi, BLE, Zigbee, Z-Wave, 6LoWPAN, NFC, WiFi Direct, GSM, LTE, LoRa, NB-IoT, and LTE-M,” *PREDICTABLE DESIGNS*, 13-Jan-2021. Available: https://predictabledesigns.com/wireless_technologies_bluetooth_wifi_zigbee_gsm_lte_lora_nb-iot_lte-m/.
- [31] M. Jain, “NFC vs. Bluetooth: First-Ever Tabularized Comparison,” *Konstantinfo*, 07-Sep-2020. Available: <https://www.konstantinfo.com/blog/bluetooth-vs-nfc/>.
- [32] S. H. Crandall, L. G. Kurzweil, and A. K. Nigam, “On the measurement of Poisson’s ratio for modeling clay,” *Experimental Mechanics*. Available: <https://link.springer.com/article/10.1007%2FBBF02327644>.
- [33] (PDF) *Determination of Elastic Modulus of Gelatin Gels by ...* (n.d.). https://www.researchgate.net/publication/279635429_Determination_of_Elastic_Modulus_of_Gelatin_Gels_by_Indentation_Experiments.
- [34] Lucien, M. A. B., Schaad, N., Steenland, M. W., & Katz, M. A. (2021, March 12). *Figure 3. The calculation of sensitivity, specificity, positive...* ResearchGate. https://www.researchgate.net/figure/The-calculation-of-sensitivity-specificity-positive-predictive-value-PPV-and_fig1_273156865.

APPENDIX A: ADC Code in Keil Uvision

```
//Header File
#ifndef ADC
#define ADC

#include <MKL25Z4.h>
#include <stdio.h>
#define PTE20 (20)
void init_ADC(void) ;
float measure_POT(void);
#endif

//.C File
#include "adccap.h"
void init_ADC(void) {
    SIM->SCGC6 |= SIM_SCGC6_ADC0_MASK;
    SIM->SCGC5 |= SIM_SCGC5_PORTE_MASK;
    // Select analog for pin
    PORTE->PCR[PTE20] &= ~PORT_PCR_MUX_MASK;
    PORTE->PCR[PTE20] |= PORT_PCR_MUX(0);
    // long sample time improves accuracy & uses less power
    ADC0->CFG1 = ADC_CFG1_ADLPSC_MASK | ADC_CFG1_ADLSMP_MASK ;
    //16 bit single-ended conversion, when DIFF=0
    ADC0->CFG1 |= ADC_CFG1_MODE(3);
    // Default settings: Software trigger, voltage references VREFH
    and VREFL
    ADC0->SC2 = ADC_SC2_REFSEL(0);
}
//consider continuous conversion, enable hardware average,
take avg of 32 samples ((2^2)^N, N=3
//ADC0->SC3 |=ADC_SC3_ADC0_MASK | ADC_SC3_AVGE_MASK |
ADC_SC3_AVGS(3);
float measure_POT(void){
    float val;
    unsigned int sample =0;
    ADC0->SC1[0] = 0x00; // start conversion on channel 0, (the
    software trigger & chan selection)
    while (!(ADC0->SC1[0] & ADC_SC1_COCO_MASK));
    sample = ADC0->R[0];
    val = (float)5*sample/0xffff;//recall 0xffff maps to max of 5v
    return val;
}
```

APPENDIX B: Serial UART Code for Bluetooth Connection

```
//Header File
#ifndef CAPSH_H
#define CAPSH_H

#include <MKL25Z4.H>
#include <stdio.h>
#include <stdio.h>
#include <stdlib.h>
#include <stdint.h>
#define Q_MAX_SIZE (256)

typedef struct {
    unsigned int Head; // Index of oldest data element
    unsigned int Tail; // Index of next free space
    unsigned int Size; // Number of elements in use
    uint8_t Data[Q_MAX_SIZE];
} volatile Q_T;

extern int Q_Empty(Q_T * q);
extern int Q_Full(Q_T * q);
extern int Q_Size(Q_T * q);
extern int Q_Enqueue(Q_T * q, uint8_t d);
extern uint8_t Q_Dequeue(Q_T * q);
extern void Q_Init(Q_T * q);
#endif



---


//.C File
#include "capshead.h"
void Q_Init(Q_T * q) {
    unsigned int i;
    for (i=0; i<Q_MAX_SIZE; i++)
        q->Data[i] = '_'; // to simplify our lives when debugging
    q->Head = 0;
    q->Tail = 0;
    q->Size = 0;
}
int Q_Empty(Q_T * q) {
    return q->Size == 0;
}
int Q_Full(Q_T * q) {
    return q->Size == Q_MAX_SIZE;
}
int Q_Size(Q_T * q) {
    return q->Size;
}
int Q_Enqueue(Q_T * q, uint8_t d) {
    uint32_t masking_state;
    // If queue is full, don't overwrite data, but do return an error
    code
}
```

```

    if (!Q_Full(q)) {
        q->Data[q->Tail++] = d;
        q->Tail %= Q_MAX_SIZE;
        // protect q->Size++ operation from preemption
        // save current masking state
        masking_state = __get_PRIMASK();
        // disable interrupts
        disable_irq();
        // update variable
        q->Size++;
        // restore interrupt masking state
        set_PRIMASK(masking_state);
        return 1; // success
    } else
        return 0; // failure
}

uint8_t Q_Dequeue(Q_T * q) {
    uint32_t masking_state;
    uint8_t t=0;
    // Check to see if queue is empty before dequeuing
    if (!Q_Empty(q)) {
        t = q->Data[q->Head];
        q->Data[q->Head++] = '_'; // empty unused entries for debugging
        q->Head %= Q_MAX_SIZE;
        // protect q->Size-- operation from preemption
        // save current masking state
        masking_state = __get_PRIMASK();
        // disable interrupts
        disable_irq();
        // update variable
        q->Size--;
        // restore interrupt masking state
        set_PRIMASK(masking_state);
    }
    return t;
}

```

APPENDIX C: Code to Execute ADC, Bluetooth data transfer & Light LEDs

```
#include <mkl25z4.h>
#include <stdint.h>
#include "capshead.h"
#include "adccap.h"

#define RX 1          //PTA1
#define TX 2          //PTA2
#define OSR 15        //over sample rate (like a pre-scaler)
#define BAUD_RATE     9600 //my communication rate on BT
#define SYS_CLOCK     20971520u //

#define MASK(x) (1UL << (x))
#define RED_LED_POS (18)          // on port B
#define GREEN_LED_POS (19) // on port B
#define BLUE_LED_POS (1)          // on port D

#define malignantTisVal 1.5
#define normalTisVal 1
#define uncertainTisVal 0.5

volatile char rxChar;
Q_T TxQ, RxQ;
float val;
int whole;
float fraction;
int decimal;
volatile unsigned long counter=0;
unsigned long millis();

void SysTick_Handler();
void UART0_IRQHandler(void);

void init_pins(void);
void init_UART(void);

void Init_RGB_LEDs(void);
void lightLED(void);

void doTxRx_task(void);
void Control_RGB_LEDs(unsigned int red_on, unsigned int green_on,
unsigned int blue_on);
void delay(int delay);

//functions
void Init_UART(void){ //select clock for uart0 (disabled by default),
MCGFLLCLK/system clk as UART0 clock
    SIM->SOPT2 |= SIM_SOPT2_UART0SRC(1);
    // clock gate UART0
    SIM->SCGC4 |= SIM_SCGC4_UART0_MASK;    //clock gate UART0
```

```

//compute set baud rate (SBR), choosing baud rate of 9600 for BT
uint8_t sbr = (uint16_t)((SYS_CLOCK)/((OSR+1) *BAUD_RATE ));
//default OSR is 15, sbr=136.5 if SYS_CLOCK =20971520u
//UART0->BDH |=((sbr>>8) & 0x1F); //generic. set only
bottom 5 bits
UART0->BDH =0; //0x0 for this calculation
UART0->BDL=sbr; //0x88 for this calculation
// Rx Interrupt enabled, Tx & RX enable
UART0->C2|=UART_C2_RIE_MASK|UART_C2_TE_MASK | UART_C2_RE_MASK;
//note: default is 8N1 if uart0->C1=0

NVIC_SetPriority(UART0_IRQn, 3);
NVIC_ClearPendingIRQ(UART0_IRQn);
NVIC_EnableIRQ(UART0_IRQn);
}

void init_pins(void){
//Clock gate port A
SIM->SCGC5 |= SIM_SCGC5_PORTA(1);
PORTA->PCR[RX] &= ~PORT_PCR_MUX_MASK; //clear mux
PORTA->PCR[RX] |= PORT_PCR_MUX(2); //set for UART0 RX
PORTA->PCR[TX] &= ~PORT_PCR_MUX_MASK; //clear
PORTA->PCR[TX] |= PORT_PCR_MUX(2); //set for UART0 TX
}

//led setup and control
void Init_RGB_LEDs(void) {
// Enable clock to ports B and D
SIM->SCGC5 |= SIM_SCGC5_PORTB_MASK | SIM_SCGC5_PORTD_MASK;

// Make 3 pins GPIO
PORTB->PCR[RED_LED_POS] &= ~PORT_PCR_MUX_MASK;
PORTB->PCR[RED_LED_POS] |= PORT_PCR_MUX(1);
PORTB->PCR[GREEN_LED_POS] &= ~PORT_PCR_MUX_MASK;
PORTB->PCR[GREEN_LED_POS] |= PORT_PCR_MUX(1);
PORTD->PCR[BLUE_LED_POS] &= ~PORT_PCR_MUX_MASK;
PORTD->PCR[BLUE_LED_POS] |= PORT_PCR_MUX(1);
// Set ports to outputs
PTB->PDDR |= MASK(RED_LED_POS) | MASK(GREEN_LED_POS);
PTD->PDDR |= MASK(BLUE_LED_POS);

//setting them off initially
PTB->PSOR = MASK(RED_LED_POS);
PTB->PSOR = MASK(GREEN_LED_POS);
PTD->PSOR = MASK(BLUE_LED_POS);
}

void Control_RGB_LEDs(unsigned int red_on, unsigned int green_on,
unsigned int blue_on) {
if (red_on) {
PTB->PCOR = MASK(RED_LED_POS);

```

```

    } else {
        PTB->PSOR = MASK(RED_LED_POS);
    }
    if (green_on) {
        PTB->PCOR = MASK(GREEN_LED_POS);
    } else {
        PTB->PSOR = MASK(GREEN_LED_POS);
    }
    if (blue_on) {
        PTD->PCOR = MASK(BLUE_LED_POS);
    } else {
        PTD->PSOR = MASK(BLUE_LED_POS);
    }
}

void lightLED(void) {
    if (whole <= malignantTisVal) {
        Control_RGB_LEDs(1,0,0); //malignantTisVal
    }
    if (whole == normalTisVal) {
        Control_RGB_LEDs(0,1,0); //normalTisVal
    }
    if (whole == uncertainTisVal) {
        Control_RGB_LEDs(0,0,1); //uncertain TisVal
    }
}

void UART0_IRQHandler(void) {
    uint8_t ch;
    if (UART0->S1 & (UART_S1_OR_MASK | UART_S1_NF_MASK | UART_S1_FE_MASK |
        UART_S1_PF_MASK)) { // clear the error flags
        UART0->S1 |= UART0_S1_OR_MASK | UART0_S1_NF_MASK | UART0_S1_FE_MASK |
        UART0_S1_PF_MASK; // read the data register to clear RDRF
        ch = UART0->D;
    }
    if (UART0->S1 & UART0_S1_RDRF_MASK) {
        // received a character...whole val
        ch = UART0->D;
        rxChar=ch; //whole=ch;
        lightLED();
        if (!Q_Full(&RxQ)) {
            Q_Enqueue(&RxQ, ch);
        } else {
        }
    }
    if ( (UART0->C2 & UART0_C2_TIE_MASK) && // transmitter
        interrupt enabled
        (UART0->S1 & UART0_S1_TDRE_MASK) ) { // tx buffer
        empty
        // can send another character
        if (!Q_Empty(&TxQ)) {
            UART0->D = Q_Dequeue(&TxQ);
        } else {

```

```

        // queue is empty so disable transmitter interrupt
        UART0->C2 &= ~UART0_C2_TIE_MASK;
    }
}

void Send_String(uint8_t * str) {
    // enqueue string
    while (*str != '\0') { // copy characters up to null terminator
        while (Q_Full(&TxQ))
            ; // wait for space to open up
        Q_Enqueue(&TxQ, *str);
        str++;
    }
    // start transmitter if it isn't already running
    if (!(UART0->C2 & UART0_C2_TIE_MASK)) {
        UART0->D = Q_Dequeue(&TxQ);
        UART0->C2 |= UART0_C2_TIE(1);
    }
}

int main (void) {
    Q_Init(&TxQ);
    Q_Init(&RxQ);
    init_pins();
    Init_UART();
    Init_RGB_LEDs();
    init_ADC();
    uint8_t buff [30]="Ashesi Embedded!";
    UART0_IRQHandler();
    //setup the systick timer
    SysTick->LOAD = (20971520u/1000u)-1 ; //configure for every half sec
    restart.
    SysTick->CTRL |= SysTick_CTRL_CLKSOURCE_Msk
    |SysTick_CTRL_ENABLE_Msk |SysTick_CTRL_TICKINT_Msk;
    unsigned long current_time =0u;
    unsigned long last_run=0u;
    unsigned long interval=1000; //1 sec

    while (1) {
        current_time= millis(); //current time
        if((current_time-last_run) >= interval){
            last_run=current_time;
            doTxRx_task();
            val=measure_POT(); //sprintf(buff,"Voltage= %5.2", val);
            whole=val;
            fraction = val-whole;
            decimal= fraction*100; //working to 2 decimal places
            sprintf(buff,"Voltage= %2d.%02d", whole, decimal);
        }
    }
}

void doTxRx_task()

```

```

{
    uint8_t buffer[80], c, * bp;
    if (Q_Size(&RxQ) == 0)
        return;    //nothing received. Exit
    //lightLED();
    //echo character sent:
    c = Q_Dequeue(&RxQ);
    sprintf((char *) buffer, "Data sent %c", c);
    // enqueue string
    bp = buffer;
    while (*bp != '\0')
    {
        //enqueue full string
        while (Q_Full(&TxQ)) ; // wait if buffer full
        Q_Enqueue(&TxQ, *bp);
        bp++;
    }
    // start transmitter if it isn't already running
    if (!(UART0->C2 & UART0_C2_TIE_MASK))
    {
        UART0->C2 |= UART0_C2_TIE(1);
    }
}

void SysTick_Handler(){
    counter++; //increases every 1ms.
    Send_String(buff);
}

unsigned long millis(){
    return (unsigned long)counter;
}

```

APPENDIX D: Bill of Materials

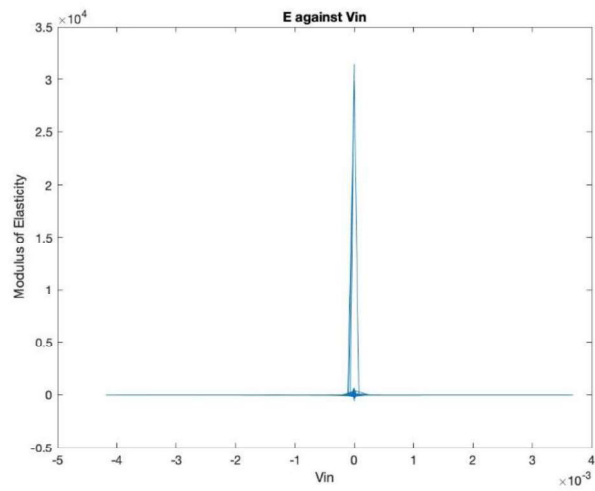
Bill of Materials					
Product Name	White Cotton Gloves	Cost	\$7.96		
Brand	Charmics				
Acquired?	Yes	Shipping cost	\$0.00		
		Total Cost	\$7.96		
Product Name	Analog Ceramic Piezo Vibration sensor(3.3/5 V)	Cost	\$7.99		
Brand	MakerHawk				
Acquired?	Yes	Shipping cost	\$25.00		
		Total Cost	\$32.99		
Product Name	Gelatin	Cost	\$4.32		(b)
Product Name	Modelling Clay	Cost	1.7		
Acquired?	No	Shipping cost	\$0.00		
		Total Cost	\$6.02		
Total			\$46.97		
GHS 261.78					

APPENDIX E:3D modeling of system using Blender



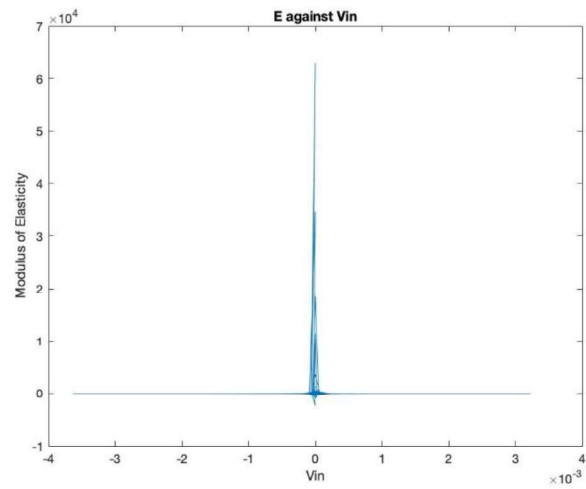
APPENDIX F: Breast Phantom 1 Only Elasticity values and graphs

Time (s)	Channel 1	Channel 2 (V)	Average	EM
-0.14998	-2.85526	-2.81625	-2.83575	-19.9315
-0.14994	-2.95023	-2.91115	-2.93086	-19.5405
-0.1499	-2.89747	-2.86211	-2.87979	-19.6268
-0.14987	-2.92209	-2.8868	-2.90445	-19.8043
-0.14983	-2.98541	-2.9503	-2.96785	-19.6507
-0.14979	-3.01355	-2.97852	-2.99604	-19.5159
-0.14976	-3.11204	-3.07377	-3.09291	-19.3249
-0.14972	-3.2246	-3.18666	-3.20563	-19.7836
-0.14968	-3.17888	-3.14433	-3.1616	-19.6797
-0.14965	-3.12963	-3.09494	-3.11228	-18.9477
-0.14961	-3.19646	-3.16196	-3.17921	-18.9419
-0.14957	-3.29496	-3.25721	-3.27608	-19.0379
-0.14954	-3.32662	-3.29249	-3.30955	-18.5887
-0.1495	-3.34772	-3.31013	-3.32892	-17.9701
-0.14946	-3.37234	-3.33835	-3.35535	-18.201
-0.14943	-3.41104	-3.37363	-3.39233	-18.7098
-0.14939	-3.32662	-3.29602	-3.31132	-18.111
-0.14935	-3.25978	-3.22546	-3.24262	-17.4466
-0.14932	-3.33365	-3.29602	-3.31483	-18.0164
-0.14928	-3.45325	-3.41243	-3.43284	-18.4017
-0.14924	-3.62209	-3.58176	-3.60193	-18.9533
-0.14921	-3.703	-3.6629	-3.68295	-19.3235
-0.14917	-3.69245	-3.65584	-3.67414	-19.397
-0.14913	-3.71355	-3.67701	-3.69528	-19.4214
-0.1491	-3.75576	-3.71934	-3.73755	-19.9239
-0.14906	-3.67838	-3.64526	-3.66182	-20.063
-0.14902	-3.75576	-3.71934	-3.73755	-19.4559
-0.14899	-3.82612	-3.78637	-3.80624	-18.9997
-0.14895	-3.97034	-3.931	-3.95067	-18.9883
-0.14891	-4.04069	-4.00156	-4.02112	-18.6805
-0.14888	-4.09697	-4.06153	-4.07925	-18.684
-0.14884	-4.03365	-3.99803	-4.01584	-18.7052
-0.1488	-3.9035	-3.87103	-3.88727	-18.321
-0.14877	-3.84722	-3.81459	-3.8309	-17.9252
-0.14873	-3.81908	-3.78637	-3.80272	-17.5848



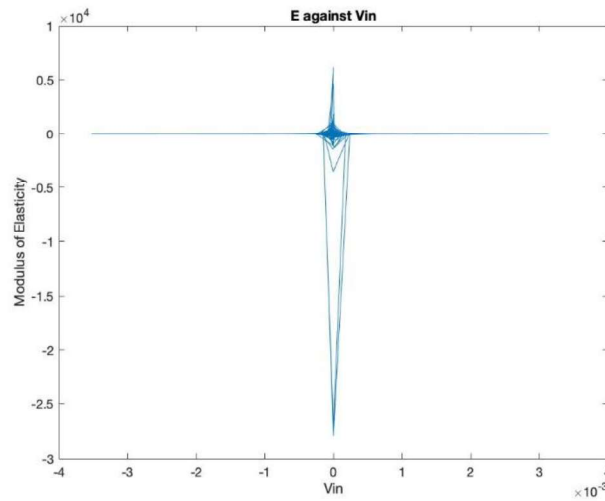
APPENDIX G: Breast Phantom 1 with tumor Elasticity values and graphs

Time (s)	Channel 1	Channel 2 (V)	Average	EM
-0.15	-1.7472	-1.7438	-1.7455	-14.656
-0.1499	-1.7824	-1.7826	-1.7825	-13.847
-0.1499	-1.8211	-1.825	-1.823	-14.554
-0.1499	-1.8774	-1.8814	-1.8794	-15.128
-0.1498	-1.9055	-1.9061	-1.9058	-14.787
-0.1498	-1.9547	-1.9555	-1.9551	-14.798
-0.1498	-2.0427	-2.0472	-2.0449	-14.686
-0.1497	-2.1236	-2.1283	-2.126	-15.419
-0.1497	-2.1728	-2.1777	-2.1753	-15.736
-0.1496	-2.2362	-2.2448	-2.2405	-15.278
-0.1496	-2.3171	-2.3259	-2.3215	-15.456
-0.1496	-2.3346	-2.3435	-2.3391	-15.297
-0.1495	-2.405	-2.4141	-2.4095	-14.932
-0.1495	-2.4824	-2.4917	-2.487	-14.447
-0.1495	-2.5281	-2.5376	-2.5328	-14.896
-0.1494	-2.4754	-2.4811	-2.4782	-15.144
-0.1494	-2.5176	-2.5305	-2.524	-14.909
-0.1494	-2.6477	-2.6575	-2.6526	-15.015
-0.1493	-2.7216	-2.7316	-2.7266	-15.781
-0.1493	-2.6864	-2.6963	-2.6914	-15.653
-0.1492	-2.7181	-2.7316	-2.7248	-15.92
-0.1492	-2.7955	-2.8092	-2.8023	-16.478
-0.1492	-2.8201	-2.8339	-2.827	-16.706
-0.1491	-2.8306	-2.8445	-2.8376	-16.714
-0.1491	-2.8095	-2.8233	-2.8164	-17.159
-0.1491	-2.8517	-2.8656	-2.8587	-17.727
-0.149	-2.9221	-2.9327	-2.9274	-16.987
-0.149	-2.9467	-2.9574	-2.952	-16.286
-0.149	-2.9362	-2.9503	-2.9432	-15.774
-0.1489	-3.0135	-3.0314	-3.0225	-15.477
-0.1489	-2.8728	-2.8868	-2.8798	-14.647
-0.1488	-2.9115	-2.9256	-2.9186	-15.069
-0.1488	-2.996	-3.0138	-3.0049	-15.368
-0.1488	-3.1718	-3.1902	-3.181	-15.79
-0.1487	-3.302	-3.3172	-3.3096	-15.977



APPENDIX H:Breast Phantom 2 Only Elasticity values and graphs

Time (s)	Channel 1	Channel 2 (V)	Average	EM
-0.15	-1.6519	-1.625	-1.6385	-13.76
-0.1499	-1.6871	-1.6568	-1.6719	-12.886
-0.1499	-1.7785	-1.7485	-1.7635	-14.088
-0.1499	-1.8348	-1.805	-1.8199	-14.695
-0.1498	-1.7398	-1.7168	-1.7283	-13.392
-0.1498	-1.7434	-1.7168	-1.7301	-13.031
-0.1498	-1.8313	-1.8014	-1.8164	-12.963
-0.1497	-1.8348	-1.805	-1.8199	-13.24
-0.1497	-1.8032	-1.7767	-1.7899	-13.014
-0.1497	-1.8981	-1.872	-1.8851	-12.809
-0.1496	-1.979	-1.9496	-1.9643	-13.106
-0.1496	-1.9755	-1.9461	-1.9608	-12.773
-0.1495	-1.9931	-1.9637	-1.9784	-12.002
-0.1495	-2.0881	-2.059	-2.0735	-11.669
-0.1495	-2.1479	-2.1189	-2.1334	-12.372
-0.1494	-2.1655	-2.1366	-2.151	-13.131
-0.1494	-2.2851	-2.2565	-2.2708	-13.407
-0.1494	-2.3906	-2.3623	-2.3765	-13.462
-0.1493	-2.4047	-2.38	-2.3923	-14.021
-0.1493	-2.5067	-2.4752	-2.491	-14.63
-0.1493	-2.5419	-2.514	-2.5279	-14.949
-0.1492	-2.5067	-2.4787	-2.4927	-15
-0.1492	-2.5454	-2.514	-2.5297	-15.334
-0.1491	-2.6017	-2.574	-2.5878	-15.589
-0.1491	-2.5806	-2.5564	-2.5685	-16.076
-0.1491	-2.6052	-2.5775	-2.5914	-16.628
-0.149	-2.6333	-2.6093	-2.6213	-15.657
-0.149	-2.6298	-2.6022	-2.616	-14.733
-0.149	-2.6122	-2.5846	-2.5984	-14.102
-0.1489	-2.6439	-2.6163	-2.6301	-13.552
-0.1489	-2.6615	-2.634	-2.6477	-13.443
-0.1489	-2.6826	-2.6551	-2.6688	-13.823
-0.1488	-2.8162	-2.7857	-2.8009	-14.421
-0.1488	-2.8866	-2.8562	-2.8714	-14.432
-0.1487	-2.8092	-2.7821	-2.7957	-13.697



APPENDIX I: Breast Phantom 2 with tumor Elasticity values and graphs

Time (s)	Channel 1	Channel 2 (V)	Average	EM
-0.14997	-1.53934	-1.48747	-1.5134	-12.5515
-0.14994	-1.49009	-1.43808	-1.46409	-10.687
-0.1499	-1.60618	-1.55096	-1.57857	-12.4134
-0.14986	-1.79261	-1.74499	-1.7688	-14.2998
-0.14983	-1.88758	-1.84024	-1.86391	-14.482
-0.14979	-1.88758	-1.84024	-1.86391	-14.1334
-0.14975	-1.96145	-1.91079	-1.93612	-13.9161
-0.14972	-2.14789	-2.10481	-2.12635	-15.4215
-0.14968	-2.16196	-2.1154	-2.13868	-15.5195
-0.14964	-2.11271	-2.06601	-2.08936	-14.331
-0.14961	-2.20417	-2.16478	-2.18448	-14.6452
-0.14957	-2.34487	-2.30236	-2.32362	-15.2094
-0.14953	-2.33784	-2.29531	-2.31657	-14.3927
-0.1495	-2.2499	-2.20359	-2.22674	-12.8185
-0.14946	-2.34839	-2.30942	-2.32891	-13.7157
-0.14942	-2.45744	-2.41172	-2.43458	-14.9064
-0.14939	-2.40819	-2.36586	-2.38703	-14.1356
-0.14935	-2.42578	-2.38703	-2.4064	-13.648
-0.14931	-2.46447	-2.42583	-2.44515	-14.3312
-0.14928	-2.51724	-2.47875	-2.49799	-14.6684
-0.14924	-2.58407	-2.54225	-2.56316	-15.1339
-0.1492	-2.60518	-2.57047	-2.58782	-15.4919
-0.14917	-2.70367	-2.66572	-2.68469	-16.0872
-0.14913	-2.79161	-2.75391	-2.77276	-16.4416
-0.14909	-2.90417	-2.87032	-2.88725	-17.4342
-0.14906	-3.12578	-3.0961	-3.11094	-18.5906
-0.14902	-3.11875	-3.08198	-3.10037	-17.6222
-0.14898	-3.05895	-3.02907	-3.04401	-16.6514
-0.14895	-3.07302	-3.04671	-3.05986	-16.2548
-0.14891	-3.10116	-3.06787	-3.08452	-15.736
-0.14887	-3.18207	-3.15607	-3.16907	-15.8999
-0.14884	-3.21021	-3.18429	-3.19725	-16.2287
-0.1488	-3.13282	-3.09962	-3.11622	-15.8326
-0.14876	-3.19262	-3.16665	-3.17963	-15.7842
-0.14873	-3.30166	-3.27601	-3.28884	-15.8984

